



Electrogeneration of hydrogen peroxide for electro-Fenton system by oxygen reduction using gold nanoparticle electrodeposited on graphite cathode

Azri Yamina Mounia*, Zerouali Djilali

Faculty of Sciences, Laboratory of Electrochemical, Department of chemistry, University of Sciences and Technology of Oran U.S.T.O., BP - 1505 el M'naouer, Oran 31000, Algeria, Tel. +213 662 32 70 19; email: myazri@yahoo.fr (A.Y. Mounia), Tel. +213 414 257 63; Fax: +213 557 5708 58; email: djizeroual@yahoo.fr (Z. Djilali)

Received 27 October 2013; Accepted 21 July 2014

ABSTRACT

In this study, the electrochemical deposition of gold (Au) onto graphite has been performed under different deposition potential conditions. These Au particles electrodeposited on the graphite were used as cathode for O₂ electrochemical reduction and H₂O₂ production in acidic solution, and the hydrogen peroxide (H₂O₂) electrogenerated on graphite modified by gold particles was used in electro-Fenton process. Results show firstly that the O₂ cathodic reduction on gold particles electrodeposited on the graphite electrode in acidic medium with two well-defined reduction waves at -300 mV/SCE and -1,300 mV/SCE; those waves indicated reduction of two O₂ electrons to H₂O₂. Secondly, the optimal cathodic potential condition for H₂O₂ generation on cathode modified was -300 mV and unmodified one was -500 mV/SCE. The electrolysis time, dissolved oxygen level, magnetic stirring, and pH were systematically studied; the hydrogen peroxide production increased with the aeration and electrolysis time and then became stationary after 2 h of electrolysis. The maximum H₂O₂ accumulation increased up to 60 mg/L with air compressed, at -300 mV. Optimized parameters (potential, oxygen level, and concentration of ferrous ions) were also applied to incinerate the Belgard EV2030 sodium salt of polycarboxylic acid. The incineration efficiency onto optimized parameters shows that 74% of Chemical oxygen demand was incinerated in the modified electrode that confirms the positive gold modification effect onto the performance.

Keywords: Electro-Fenton; Au particles; Oxygen reduction; Hydrogen peroxide

1. Introduction

The wastewater biological treatment process is more economic than other treatment. However, some industrial effluents are known to contain non-biodegradable organic substances, and biological processes become inadequate. For several years, advanced oxidation processes (AOPs) have been suggested as a

wastewater attractive alternative treatment containing such substances.

AOPs are environmentally friendly techniques for water remediation, and they are based on the *in situ* generation of hydroxyl radical (OH[•]), which is very strong ($E^{\circ} = 2.8$ V/SHE) and able to non-selectively mineralize organic pollutants into CO₂ and H₂O and inorganic ions. The Fenton process is one of the AOP and has been widely applied to remove organic matter

*Corresponding author.

as pre-treatment or post-treatment process in biological treatment.

During the Fenton reaction, hydrogen peroxide is catalyzed by ferrous ions to produce hydroxyl radicals [1–3].



This reaction is propagated from ferrous ions regeneration mainly by the reduction of the produced ferric species with hydrogen peroxide [4].



The hydroxyl radicals produced are capable to oxidize wide range of organic compounds. However, in the Fenton chain reactions, the rate constant of reaction (1) is between 53 and 76 L mol/s [5–8], while in reaction (2), it is only 0.01 L mol/s [4]. This means ferrous ions are consumed more rapidly than they are produced. In addition, ferrous ions can also be rapidly destroyed by hydroxyl radicals with the rate constant in the range of $3.2\text{--}4.3 \times 10^8$ L mol/s [8,9].



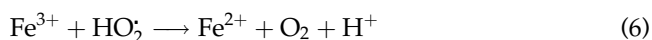
Therefore, more ferrous ion dosage is needed to keep the moderate hydroxyl radicals production. This results in the large amount of ferric hydroxide sludge during neutralization stage of Fenton process, which requires additional separation process and disposal [10].

Nowadays, electrochemical AOP are proposed as wastewater treatment option [11–13]. In this technology, the electricity is used to oxidize organic material resulting in an environmentally friendly process that does not use harsh oxidizing agents or chemical products [14]. Among electrochemical AOP are considered as one of electrochemical techniques that has attracted great attention of wastewater treatment [14–17], the electro-Fenton is an environment-friendly method owing to its ability to produce *in situ* H_2O_2 by O_2 cathodic reduction in acidic medium (3) [17], thus avoiding acquisition, shipment, and storage of H_2O_2 . The hydrogen peroxide (1.77 V) is a metastable molecule with high disinfecting and oxidizing properties [18].



The combination of H_2O_2 (Eq. (4)) and Fe^{2+} produces hydroxyl radicals (Eq. (1)); Fe^{3+} generated from

Fenton's reaction (Eq. (1)) or present in the medium, revert to Fe^{2+} by different reduction processes involving H_2O_2 or intermediate organic radicals and through the direct Fe^{3+} cathode reduction to Fe^{2+} , that allows for catalytic propagation of Fenton's reaction (Eqs. (5)–(7)). Moreover, there is no production of iron sludge during this process, and consequently, no subsequent disposal problem have been found [19] unlike the Fenton reaction.



The electro-Fenton process does not involve the use of harmful chemical reagents because Fe^{2+} ions and H_2O_2 and hydroxyl radicals (OH^\bullet) produced are not toxic and are more environment friendly [20]; the electricity as a clean energy source is used in the process, so the overall process does not create secondary pollutants. In addition, the electro-Fenton reduces the transport costs with H_2O_2 concentration handling, and it regenerates Fe^{2+} more effectively.

Variables such as selection of electrode materials usually used in the cathodes preparation mainly with graphite [21], reticulated vitreous carbon, mercury [22], and carbon felt have an important role to assure the efficiency of this process [23]. The selection of cathode material and cathode procedure preparation influences remarkably its electrochemical performance and the hydrogen peroxide production stability. For example, many researchers in order to enhance cathode activity prepare the cathode using the carbonaceous material modified with inorganic ions or organic group. Wang and Wang [24,25] prepared Pd/C gas diffusion cathode with palladium-coated activated carbon powder and applied it in the electrochemical degradation of 2,4-dichlorophenol and 4-chlorophenol aqueous solution. The result showed that removal ratios of contamination were higher using the Pd/C cathode than using unmodified activated carbon powder cathode. Lu et al. [26] studied the electrocatalytic reduction of dissolved oxygen at the glassy carbon electrodes modified with four kinds of different metal–porphyrin complexes in oxygen-saturated aqueous solutions. The result revealed that all studied complexes could catalyze the two-electron reduction of dissolved oxygen. Forti et al. [27] also studied the electrochemical synthesis of hydrogen peroxide on oxygen gas-fed graphite PTFE cathode modi-

fied by 2-ethylanthraquinone. The result showed that hydrogen peroxide formation rate on the cathode was enhanced greatly in the presence of organic redox catalyst, and the over-potential for reduction shifted toward a more positive. El-Deab et al. [28] reported that electrochemical reduction of oxygen on gold nanoparticle electrodeposited glassy carbon electrodes: Au nano/GCE, and the result of these studies indicates a remarkable separation of two peaks, the late correspond to the two steps of electro reduction of O_2 to H_2O through H_2O_2 based on the above research, and the results show that these electrochemical systems should generate hydrogen peroxide and require modification to be more suitable for practical wastewater treatment and easier to scale up. Furthermore, the cathode should be also easier to be fabricated and more enduring to reduce treatment costs.

In this work, the electrochemical deposition of Au particles onto graphite is performed under different deposition potentials and fixed deposition time. Au particles on graphite electrode are used as cathode for electrochemical reduction of O_2 in acidic solution H_2SO_4 at pH 3, and experiments series were performed to test the activity of the cathode made with Au nano/GCE for the hydrogen peroxide generation.

Procedure of the cathode influences remarkably its electrochemical performance and the hydrogen peroxide production stability, for example, many researchers in order to enhance cathode activity prepare the cathode using the carbonaceous material modified with inorganic ions or organic group.

Many industries produce large biorefractory wastewater quantities that contain organic matter and salt. The practice of discharging exhausted chemical compounds has negative impact on environment due to high organic loading; they cause serious health risks because of the toxicity and carcinogenic and mutagenic properties of biorecalcitrant compounds and their by-products. The Belgard EV 2030 is an anti-scalant/antifoulant, from thermal desalination of water treatment plant, used also in cooling towers in petrochemical refineries to reduce or prevent scale formation on transfer equipment [29]. It is a multifunctional product based on polycarboxylic acid chemistry. From the Belgard EV 2030 analysis result, it is considered toxic if mixed with other chemical compounds.

The main objective of this study is to develop electro-Fenton process at laboratory scale and to evaluate its performance in treating Belgard EV 2030. The degradation of Belgard was investigated in a modified EF system with Pt anode and Au nano/GCE.

2. Experimental

2.1. Chemicals

Belgard 2030 industrial pollution was used as refractory molecular whose chemical formula is sodium salt of polycarboxylic acid, and its structure is shown in Fig. 1. All other chemicals, including sulfuric acid, H_2SO_4 ; sodium hydroxide, NaOH; anhydrous sodium sulfate, Na_2SO_4 ; hydrogen tetrachloroaurate, $HAuCl_4$ 99%; heptahydrate ferrous sulfate, $FeSO_4 \cdot 7H_2O$; anhydrous ferric sulfate, $Fe_2(SO_4)_3$; sulfate titanium (IV), $Ti(SO_4)_2$; potassium dichromate, $K_2Cr_2O_7$; ammonium iron(II), sulfate hexahydrate (Mohr salt), $Fe(NH_4)(SO_4)_2 \cdot 6H_2O$; silver sulfate, Ag_2SO_4 ; and sulfate mercury, $HgSO_4$, were of analytical grade, and deionized water is used.

2.2. Electrochemical cell

All chemicals used in this study were analytical grade and used without further purification. The graphite comes from the electrical industrial (SONEL-GAZ, the Algerian Electrical and Gas Company), composed by carbon and a silicium fraction, and the electrode has the tubular form and is used in our study as an electrode modified by gold particles deposit and the hydrogen peroxide production and finally for organic pollution degradation.

The electrochemical experiment of deposition of gold particles on the industrial graphite is performed in an undivided cell of three electrodes. The cell was connected to potentiostat Amel 433. The industrial graphite was used as working electrode (0.07 cm^2 area), the Pt (2 cm^2 area) as a counter electrode, and saturated calomel electrode as a reference electrode.

The hydrogen peroxide electrochemical generation experiments and degradation test were carried out in a double compartment cell; the anodic compartment consists of a glass-frit bottom which allows its

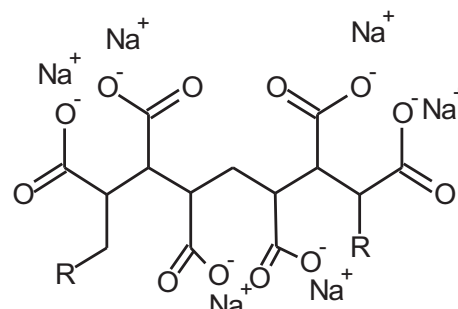


Fig. 1. Molecular structure of Belgard EV 2030.

separation from the cathodic compartment. The cell was filled with 0.5 M Na₂SO₄ aqueous solution used as support electrolyte. The pH was adjusted to 3 by using sulfuric acid and sodium hydroxide prior to electrolysis.

2.3. Analytical procedures

Scanning electron microscopy analysis of the gold on graphite was carried out using HITACHI model TM 1,000 at an acceleration voltage of 10KV with a variable pressure system and X-ray analysis incorporated. The X-ray microanalysis system HITACHI TM swift ED is controlled by a PC running windows (University of Boubker Belkaid, Department of Physics, Tlemcen).

The hydrogen peroxide concentration during electrogeneration process in the cell was monitored by UV–vis Spectrophotometer SAFAS 320G using the absorbance titanium (IV) sulfate of Ti⁴⁺-H₂O₂ orange complex at 410 nm. The current efficiency (CE) for H₂O₂ production was defined as follow [17]:

$$\eta = \frac{nFC_{\text{H}_2\text{O}_2}V}{\int_0^t Idt} \times 100\% \quad (8)$$

where n is the electrons number transferred for oxygen reduction to H₂O₂, F is the Faraday constant (96,486 C/mol), $C_{\text{H}_2\text{O}_2}$ (mol/L) is the concentration of H₂O₂, V is the bulk volume (L), I is the current (A), and t is time (s).

Chemical oxygen demand (COD) was measured according to French AFNOR norm. Samples withdraw during electro-Fenton processing were filtered with a Millex-GV Millipore hydrophilic membrane with 0.22 μm pore diameter [16].

First, the organic matter was oxidized by potassium dichromate in the presence of silver sulfate (catalyst) and mercury sulfate for a prior 2 h at 148 °C. COD was calculated from the following equation:

$$\text{COD}(\text{mg O}_2/\text{L}) = 8,000 \left(\frac{V_{\text{MS blank}} - V_{\text{MS sample}}}{N_{\text{MS}}/V_0} \right)$$

where $V_{\text{MS blank}}$ and $V_{\text{MS sample}}$ are the standard Mohr salt solution volumes using the blank and sample, respectively, N_{MS} is the Mohr salt normality, and V_0 is the sample volume.

3. Results and discussion

Our study is initially focalized on electrodeposition of Au particles on graphite, and the potential deposition is examined in order to study its behavior in the electrochemical O₂ reduction in acidic solution

0.5 M H₂SO₄. The second part is devoted to the H₂O₂ production on graphite modified by Au particles and finally to organic pollution degradation (Belgard EV 2030) by EF process. Our characterizations are aimed at elucidating the Au microcrystal existence and estimating the particle size of Au microcrystal, because both graphite substrate and Au microcrystal activate electrode materials and allow the double oxygen reduction.

3.1. Au particles deposition

Au particles were deposited on graphite from 0.5 M H₂SO₄ solution of HAuCl₄ by employing a scan of potential from 1,000 mV/SCE to potential -1,000 mV/SCE. The electrochemical behavior of this system is described in Fig. 2.

The Fig. 2 shows the current–potential curve for cyclic voltammetric experiments in 5.8×10^{-4} M HAuCl₄ in 0.5 M H₂SO₄ solution at graphite electrode.

When the potential becomes less than 900 mV/SCE, reduction peak appears at around 700 mV/SCE and a shoulder at a potential of about 500 mV/SCE. The first reduction peak corresponds to the reduction of adsorbed tetrachloroaurate anions [30].

The shoulder is attributed to the reduction of Au (III) to Au (0) and the gold nucleation [31] on the electrode surface. Subsequently, the current intensity decreased until it reaches a minimum, and this indicates that the process becomes limited by ion transport tetrachloroaurate in boundary layer near the electrode.

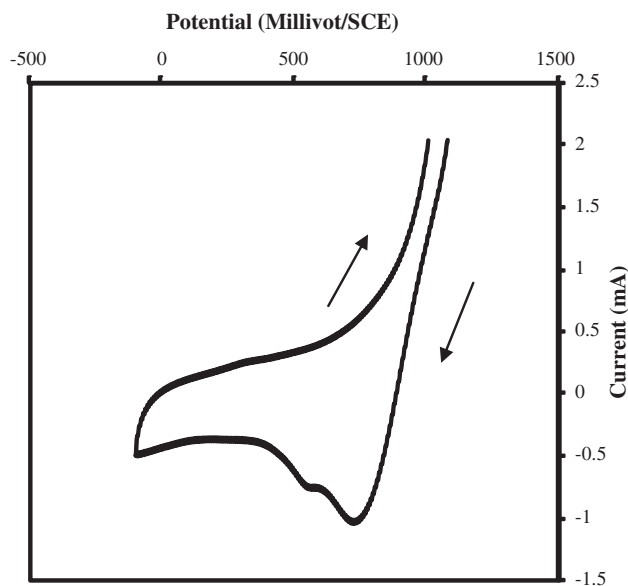


Fig. 2. Cyclic voltammogram recorded on electrode of graphite. $V_s = 400$ mV/s.

A low potential of 0 mV/SCE corresponds to the H^+ cations reduction in solution. An anodic current “crossover”, signifying metal nucleation and growth, is not observed at the scan rate employed in Fig. 2 [32,33]. Voltammetry, which more closely resembles the reported current–potential curves for nucleation and growth, is observed at scan rates slower than 5 mV/s. Furthermore, no anodic current is observed on the reverse sweep indicating the irreversibility of the $AuCl_4^-$ reduction. Therefore, we can estimate that the potential range in which only the reduction of gold is from 700 to -100 mV/SCE.

3.2. Characterization of the Au deposits

The typical [SEM] micrographs of the Au nanoparticles electrodeposited onto the graphite under differ-

ent potentials are shown in (Fig. 3), and the micrographs show a circular bright spots surrounded by a textured background of darker graphite substrate and the effect of electrodeposition potential on Au microcrystal distribution and sizes. For the potentials E900, 700 and 500 mV/ECS (typically ~ 50 – 200 nm), no differences exists. The crystallites distribution is substantially the same; however, at -500 mV/ECS, the Fig. 3(d) shows that the crystallite distribution on the graphite surface is more important, and the particles diameters estimated are at about (50–250 nm).

In order to evaluate the real surface area of the Au nanoparticles electrodeposited on the graphite, the characteristic voltammetry response of each electrode is measured in 0.5 M H_2SO_4 . First, the gold was deposited on graphite by electrodeposition in 0.5 M H_2SO_4 solution of 5.8×10^{-4} M $HAuCl_4$ at different

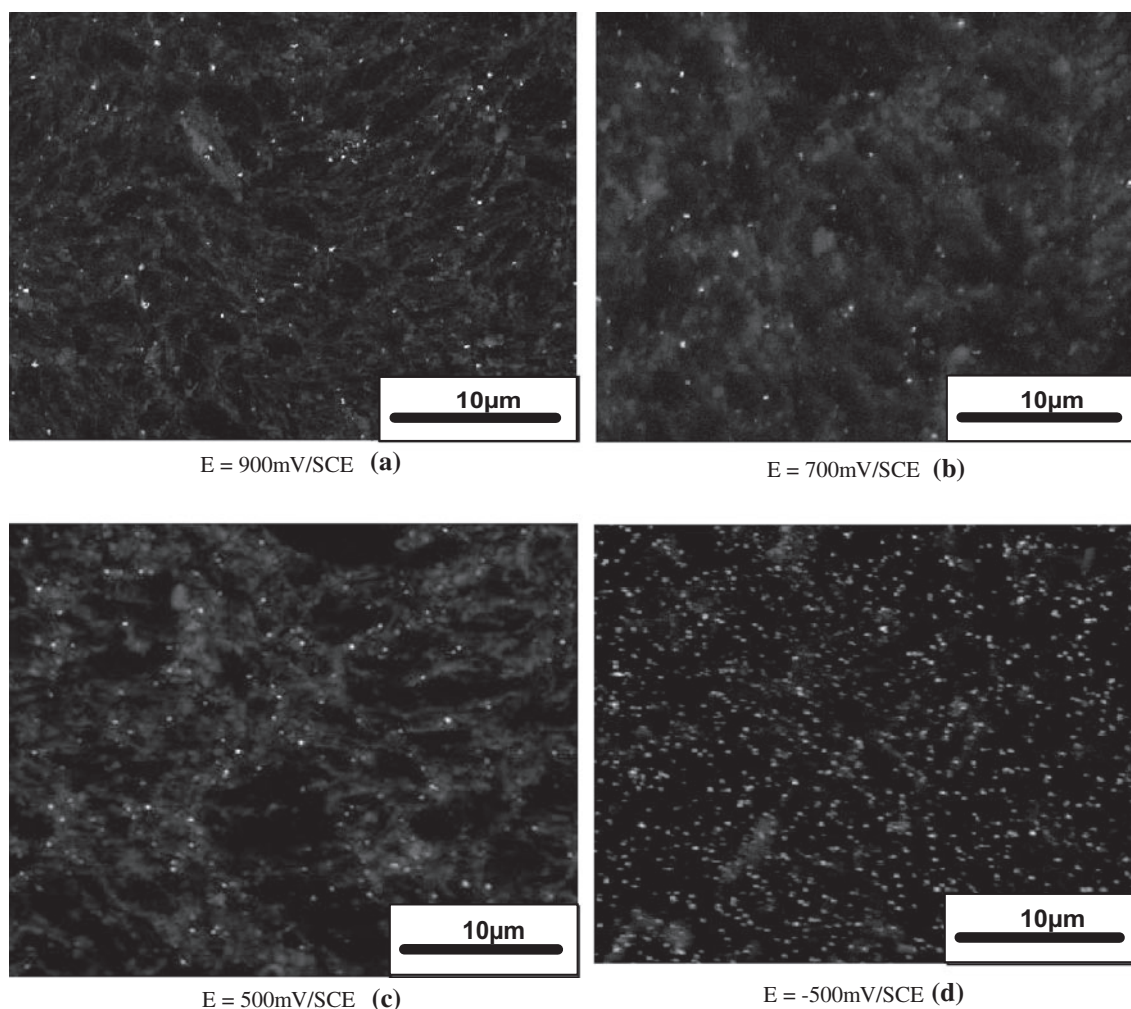


Fig. 3. SEM images of electrochemically deposited gold crystallite on graphite. Deposition potential series: E900, E700, E500, and E-500 mV/SCE; deposition time 600 s. These surfaces show the presence of microcrystalline.

potentials E900, E700, E500, and E-500 mV/SCE with a deposition time of 600 s, finally, swept linearly from 900 to 0 mV/SCE at scan rate 100 mV/s as shown in Fig. 4.

Fig. 4 shows a linear cathodic reduction response, and the presence of the reduction peak current at $\sim +400$ mV/SCE reflects the Au loading on the graphite for such imposition potentials. The real surface area of the Au loading was estimated by calculating the amount of charge consumed during the reduction of the Au surface oxide monolayer using a reported value of $489 \mu\text{C}/\text{cm}^2$ [34]. Table 1 summarizes the loading characteristics of the Au nanoparticles electrodeposited on the graphite under different potential of electrodeposition.

3.3. Influence of deposition potential on O_2 reduction

To investigate the electrochemical modification effects, on electrocatalytic activity of cathodes toward the oxygen reduction reaction (ORR), the linear sweep voltammetry was carried out on graphite electrode, modified, by gold particles at different deposition potentials extracted from the curve Fig. 2: 900, 700, 500, and -500 mV/SCE, as shown in Fig. 5. This figure reflects two important catalytic features of the graphite electrode loaded with the Au nanoparticles (i) a significant positive shift and splitting of the O_2 reduction peak from -500 mV (in the case of the graphite electrode) to -150 and $-1,300$ mV vs CSE. (ii) An increase in the peak current.

In fact, the curves corresponding at ORR tended to have two well-separated electrochemical reduction peaks. It has been observed on graphite loaded of Au, in O_2 -saturated pH 3 solution, a potential of about -300 to $-1,300$ mV/SCE, for depositions of potential

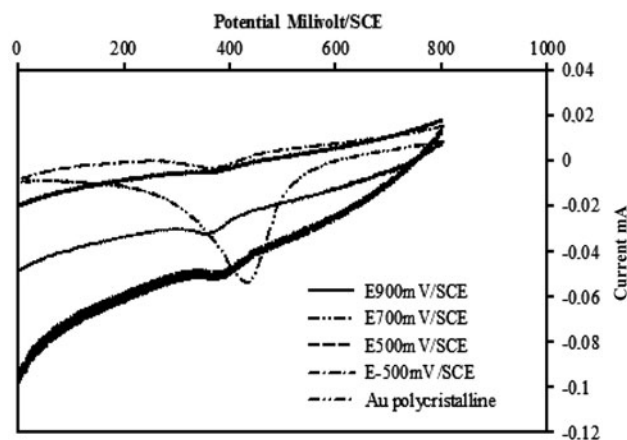


Fig. 4. Linear sweep voltammograms behavior of Au oxides in $0.5 \text{ M H}_2\text{SO}_4$.

$E = 900$ mV/SCE and $E = 700$ mV/SCE also $E = 500$ mV/SCE. For the potential $E = -500$ mV/SCE, this separation becomes less obvious, probably at the increasing of gold coverage 33% (Table 1) which decrease the activity of the graphite electrode.

In case of the curve $E = 900$ mV, we find that the first O_2 reduction peak is due to the two-electron reduction of O_2 to H_2O_2 in the range potential -100 to 500 mV/SCE following the reaction (9)



The second range of potential $-1,000$ to $-1,500$ mV/SCE is assigned to H_2O_2 reduction formed during the first step to H_2O that takes place as:



A significant positive shift of reduction peak potentials and a concurrent increase in the current peak can be obtained with a very minute amount of Au (1.5×10^{-6} mg). Without the use of any redox mediator, this has been achieved. The Au nanoparticles electrodeposited on graphite are considered as microdisk array-type electrode (see SEM), at which the diffusion layers at individual Au nanoparticles overlap with other form of a linearly expanding diffusion region [16] as can be expected by comparison of the average distance between the Au nanoparticles (~ 0.05 – $0.1 \mu\text{m}$) and the diffusion layer ($\delta \sim 0.766$ cm), under the experimental conditions of Fig. 5. Consequently, the linear sweep voltammetry response (the shape of the O_2 reduction wave) of this electrode is similar to that observed at the graphite with same apparent geometric surface area. These results suggested that the potential of deposition $E = 900$ mV and $E = 700$ mV could have significant impact to the catalytic activity toward O_2 reduction and therefore in the H_2O_2 production and EF process.

3.4. H_2O_2 production

The effects of graphite modification by Au nanoparticles on electrocatalytic activity of H_2O_2 production were investigated by the experiments performed choosing a new electrode of graphite loaded of gold with electrodeposition at $E = 700$ mV/ECS, time of deposition of 600s, as working electrode.

Fig. 6 shows the yields of hydrogen peroxide and current efficiencies at different potentials that were chosen according to the results of linear sweep voltammetry. The H_2O_2 yields at the potentials ranging from -100 to -900 mV were 17, 30, 59, 31, 25,

Table 1

Characterization of the Au loading on graphite under different potentials electrodeposition

Potential of deposition mV/ECS	Au particles amount deposited mg (10^{-6}) ^a	Q μC	Average surface area of Au $\text{cm}^{2\text{b}}$	Au coverage %	Particle size range/nm
900	1.5	0.0044	0.0089	13	50–100
700	0.85	0.0025	0.0051	7	50–100
500	1.2	0.0035	0.0071	10	200
–500	4	0.0113	0.023	33	50–250

^aAs calculated from the $i-t$ curve during the potential imposed.

^bAs estimated from the charge consumed for the reduction peak of the surface oxide monolayer of Au (the peak at 400 mV in Fig. 4) using a reported value of $489 \mu\text{C cm}^{-2}$.

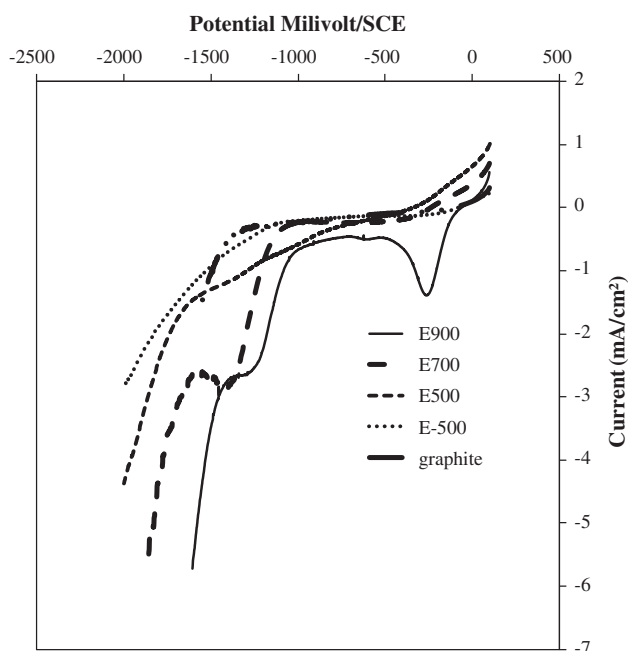


Fig. 5. Linear sweep voltammograms response for O_2 reduction at Au electrodeposited on graphite at different potential scan rate 20 mV/s .

10, 9, 5, and 3 mg/L, respectively. It indicates that the H_2O_2 accumulation increases initially with increasing cathodic potentials, and when the applied potential reaches -300 mV , the highest H_2O_2 accumulation is achieved. When the potential exceeds the optimum, H_2O_2 accumulation is declined as shown in Fig. 6(b). The H_2O_2 production current efficiencies at the applied cathode potential ranging from -100 to -900 mV were 30, 40, 70, 40, 24, 20, 15, 10, and 3%, respectively. It can be explained by the fact that, firstly, the competitive reactions such as H_2O production processes were improved after chemical modification, which become more remarkable with the increasing cathodic potentials, and H_2O_2 accumulation

inhibition, and secondly, the current in the system increases with increasing potentials; as a result, the current efficiency decreases considerably. When the cathodic potential becomes more negative than -300 mV , the side reactions corresponding to H_2O_2 decomposition become dominant, which resulted in decreased yields and efficiencies of H_2O_2 production.

3.5. Electrolysis and aeration time effect

Aeration effect before and during the electrolysis on hydrogen peroxide production was tested with potential $E = -300 \text{ mV/SCE}$. A Na_2SO_4 solution at 0.5 M and $\text{pH } 3$, magnetically stirred, was used in this experiments.

The results in Fig. 7 shows two parts: a rapid increase and a stabilization of concentration of hydrogen peroxide after 2 h.

The stabilized production of hydrogen peroxide is probably due to equilibrium between production and decomposition of hydrogen peroxide. The diagram Pourbaix's of hydrogen peroxide [35] shows instability domains of hydrogen peroxide, which can be oxidized to form oxygen or reduced to form H_2O . The plateau of Fig. 7 indicates that the production and decomposition occur simultaneously after two hours of electrolysis. The decomposition becomes higher, and the production increases slightly.

In the cathodic reduction of dissolved oxygen, oxygen is transferred from the gaseous phase to the aqueous phase, and the dissolved oxygen is transferred from the bulk aqueous solution to the cathode surface. The oxygen, which is adsorbed on active cathodic sites, is reduced to hydrogen peroxide. Hence, the mass transfer rate of oxygen from the gaseous to the aqueous phase is enhanced when the oxygen aeration time increases; until the solution is saturated with air oxygen, after 2 h of sparging, oxygen peroxide concentration did not increase.

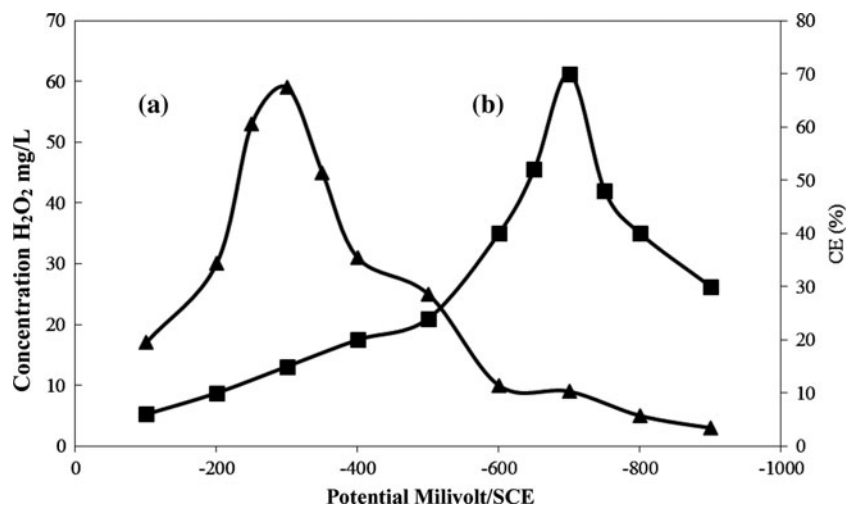


Fig. 6. The effect of the applied potentials (SCE) on (a) the yields of H₂O₂ and (b) current efficiency. Condition: using graphite Au electrode $E = 700$ mV/SCE, 0.5 M Na₂SO₄, pH = 3, O₂ air compressed. Time of electrolysis = 2 h.

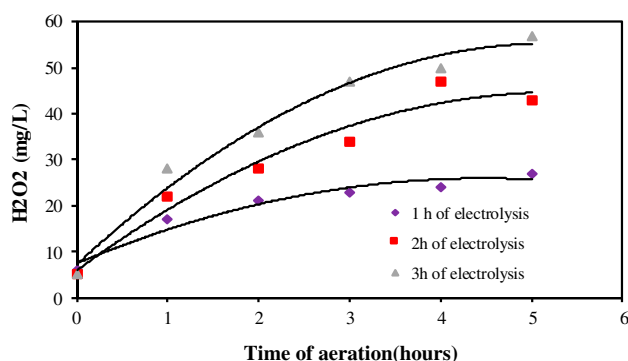


Fig. 7. Effect of aeration time.

3.6. pH effect

Electro-Fenton reaction is generally performed in acidic conditions with pH values between 2 and 4. The optimum pH value was 2.8 for hydroxyl radical production [36], ferric species begin to precipitate as ferric hydroxides at higher pH values. Furthermore, ferric species form stable complexes with H₂O₂ at lower pH values. Here, we have investigated only the effect of pH on the H₂O₂ electrogeneration using graphite modified with gold as cathode in Na₂SO₄ solution at 0.5 M, and pH values between 2 and 9 by adding of H₂SO₄ or NaOH in the absence of ferric or ferrous ions. It can be seen in Fig. 8(a), that there is a maximum H₂O₂ concentration value at pH 3 after 120 min of electrolysis. However, below pH 3, the maximum H₂O₂ concentration value was 27 mg/L. This could be explained by the formation of oxonium ion (H₃O₂⁺) [37,38], which enhanced the stability of

H₂O₂. At the same time, a low pH also promotes hydrogen evolution according to reaction (12), and then reduces the number of active sites for generating hydrogen peroxide [39].



Above a pH of 3, the values of H₂O₂ concentration decreases due to insufficient protons. These results indicate that pH 3 is an optimal condition, and this is confirmed by several authors. Fig. 8(b) shows that I stabilizes rapidly after the beginning of electrolysis. A steady-state condition is rapidly reached because a constant dissolved oxygen concentration is maintained in solution. The influence of initial pH on the electro-Fenton system was remarkable, because the ferric species began to precipitate as ferric hydroxides at higher pH values, which made it more difficult to establish a good redox system between the H₂O₂ and Fe²⁺/Fe³⁺.

3.7. Support electrolyte concentration effect

Electrogeneration of H₂O₂ was examined at different concentration of supporting electrolyte from 0.05 to 0.9 mol/L of Na₂SO₄, at pH 3 with cathodic potential of -300 mV/SCE. From Fig. 9, it could be concluded that the electrogeneration of H₂O₂ is weakly affected by change of supporting electrolyte concentration whose role is to decrease the ohmic resistance of the solution and eliminate the migration current Im. Overall current is given: $I = I_m + I_d$.

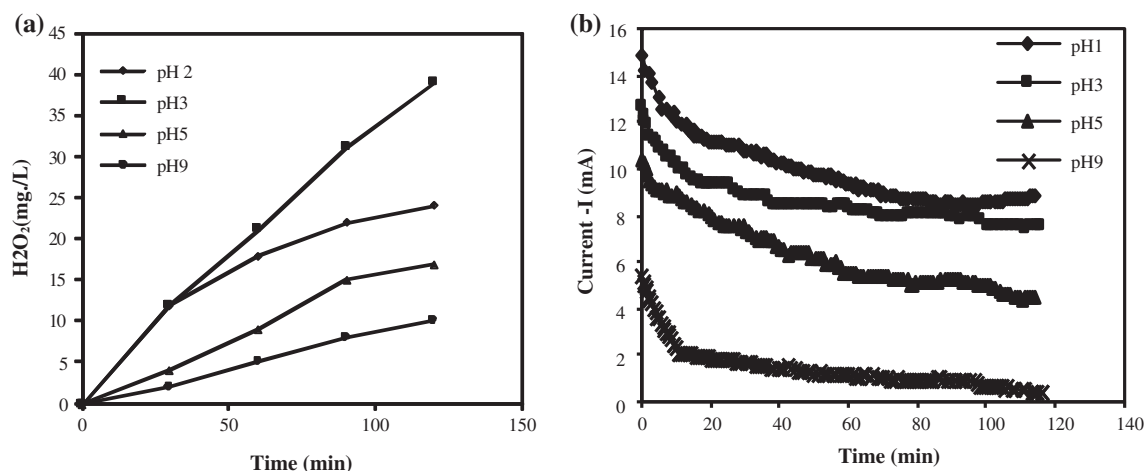


Fig. 8. H₂O₂ Generation at various applied pH: (a) accumulated concentration; (b) current. Experimental conditions: aeration time 1 h, electrolysis time 120 min and $E = -300$ mV/SCE.

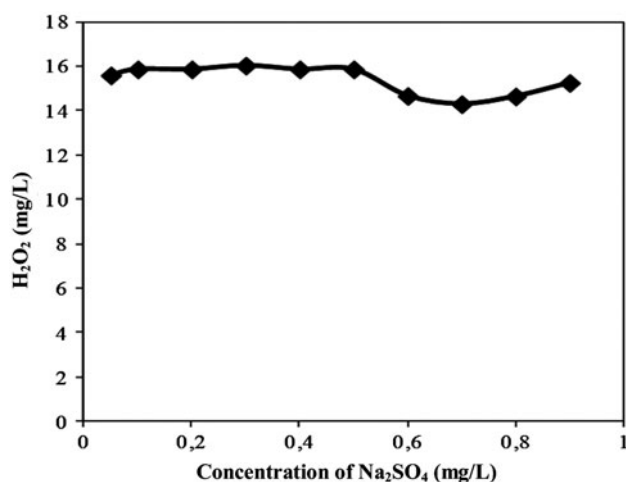


Fig. 9. Effect of Na₂SO₄ concentration in H₂O₂ electrogeneration. Experimental conditions: aeration time 1 h, electrolysis time 120 min and $E = -300$ mV/SCE.

This current is eliminated by the highly acidic solution with pH 3, and electrical migration transport phenomenon is provided essentially by the protons whose electrical mobility is much higher than that of sodium ions. However, the addition of supporting electrolyte helps to improve the solution conductivity characteristics.

3.8. Optimization of Belgard EV 2030 incineration parameters:

The indirect incineration of polycarboxylic sodium salt was performed using a galvanostatic experimental device. A DC generator LEYBOLDS 15/20 V was used

as a current source, and the graphite modified with gold particles and platinum were used as cathode and anode, respectively, and a digital ampere meter and millivoltmeter were used for current and potential measurements.

Na₂SO₄ solution at 0.5 M and pH 3 air saturated, and current $I = 0.5$ mA corresponding substantially to H₂O₂ production potential on modified graphite electrodes were used for all experiments. The solution was magnetically stirred and aerated during the electrolysis; the pH was adjusted to 3 by adding H₂SO₄ and NaOH. The incineration was controlled by COD analysis hourly. The effect of ferric ion concentration was experimented.

3.9. Ferric ion concentration effect:

Fig. 10 shows the effect of ferric ion concentration on the degradation. After 3 h of treatment with Pt anode, the initial of Belgard EV 2030 concentration with about 1,066–1,100 mg of O₂/L at 0.5 mA of current applied, the pH of the solution was adjusted at 3.

In the absence of ferric ions, only 6% of COD depletion was obtained, after 3 h of electrolysis because the main oxidant was the electrogenerated H₂O₂ that has a limited oxidation power.

In contrast, in the solution containing Fe³⁺ ions, the Belgard EV 2030 oxidation is accelerated because of the formation of OH[•] radicals, according to Fenton's reaction Eq. (1). The removal reaches the highest value at the concentration 224 mg/L.

A gradual increase in COD abatement can be observed when Fe³⁺ content increases, leading to a final mineralization of 8.1, 9.3, 12, 20, and 34% for 5.6, 11.2, 56, 112, and 168 mg/L, respectively (Fig. 10(b)),

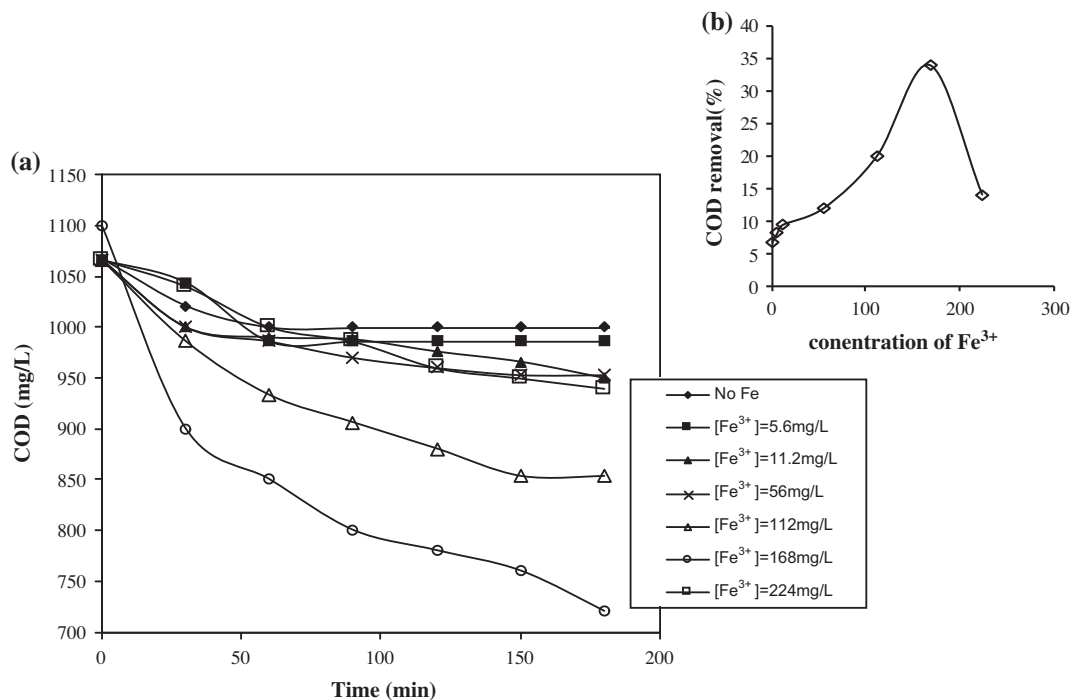


Fig. 10. Influence of the Fe³⁺ concentration on COD evolution during the electrolysis of Belgard EV 2030 degradation.

and the COD decreases to a concentration of 224 mg/L where a reduction of 14% was recorded.

However, the increase of ferric ions concentration to 224 mg/L does not bring further improvement on the COD removal. It has been reported that an excess of ferric ions would consume hydroxyl radicals by the following oxidizing reaction: [37,40,41]



Consequently, the optimal Fe³⁺ concentration for Belgard EV 2030 degradation is 168 mg/L. This concentration is used for the following experiment.

3.10. Incineration of Belgard EV 2030:

The organic pollutants, such as atrazine, phenol and derivatives, and various insecticides and pesticides, have benefited the many publications that report their degradation by the Fenton process and techniques that result in, while the oxidation of the salt sodium polycarboxylic acid by an advanced oxidation method has not been systematically studied. We did not find any data on this subject in the literature. We have therefore experimented this molecule with the electro-Fenton process using a new cathode

material based on gold nanoparticles, in order to improve the electrocatalytic performances of ORR. This improvement is based on the bielectronic reduction of the O₂ to H₂O₂, without inducing parasite reactions such as transforming H₂O₂ to H₂O, or hydrogen evolution.

The electrocatalytic performances of graphite modified with gold nanoparticles in electro-Fenton system were evaluated by degradation of 1,000 mg d'O₂/L Belgard EV 2030.

This experiment represents the application of the optimized parameters of Belgard EV 2030 indirect incineration contained in an aqueous solution acidified to pH 3. The solution was first aerated by air insufflation compressed for 2 h and then electrolyzed for 1 h, in order to produce and accumulate hydrogen peroxide. The solution was magnetically stirred. As shown in Fig. 11, the electrocatalytic activities of cathode were investigated under the modified and unmodified graphite, respectively. We can see that 14% of Belgard rate was removed after 20 h of treatment on cathode of unmodified graphite, while a higher rate of 74% was recorded for modified graphite after 10 h of treatment. This improvement of the electrocatalytic activity of modified graphite can be explained as follows: After, electrodeposition of gold on graphite electrode, the current response, under the applied potential, and electron transfer process were obviously enhanced,

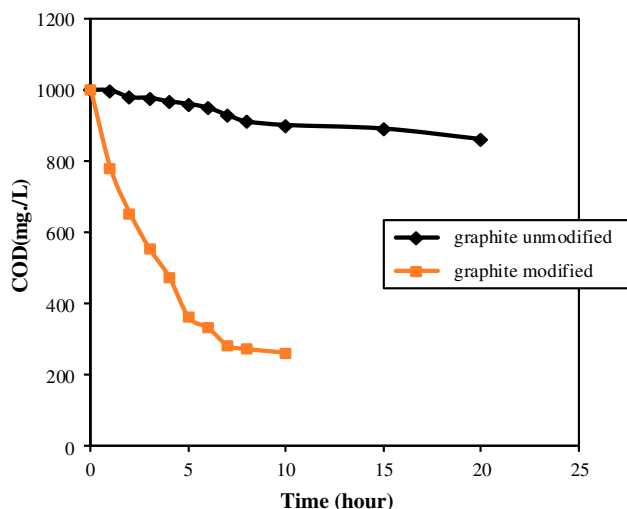


Fig. 11. Evolution of COD with time of electrolysis. Experimental conditions: $I = 0.5$ mA, $\text{Fe}^{3+} = 168$ mg/L, 0.5 M Na_2SO_4 , pH = 3, O_2 air compressed.

which could promote the reduction of Fe^{3+} to Fe^{2+} . Moreover, H_2O_2 production for modified cathode also increased, which could compete with the hydrolysis and promote the redox system between H_2O_2 and $\text{Fe}^{2+}/\text{Fe}^{3+}$ and thus improve the electro-Fenton process.

The chemical nature of the molecule experimented has an important role in AOP; indeed, the Belgard proves to be a difficult molecule to degrade with the electro-Fenton method where the very long time of the electrolysis is because of the chemical nature of Belgard, which is a carboxylic polymer. Generally, the hydroxyl radicals have relatively low reactivity to the aliphatic compounds such as organic acids, which are by-products of oxidation [16] of the small degradation, even with the modified electrode as in this case.

4. Conclusion

In this work, we demonstrated that the electro-Fenton process using graphite electrode modified with nanostructured gold constitutes a promising approach for removal of Belgard EV 2030 in industrial effluent. In fact, a simple chemical method was used to modify the graphite electrode. The results showed that modified samples have much higher electrocatalytic activity toward the ORR than the pristine one. Different compositions of gold-graphite system, by electrodeposition technique, were studied. The optimal potential of deposition is at $E = -700$ and -900 mV/SCE. In these potentials, the gold particles are reduced to the size of nanometer and improve the electroactivity toward ORR with two well-separated reduction peaks in

polarization curve, and those two peaks indicate to the two-step-four-electron reduction of O_2 to H_2O_2 then H_2O_2 to H_2O . The maximum accumulation of H_2O_2 is obtained at -300 mV/SCE, in Na_2SO_4 aqueous solution at 0.5 M and pH 3, after 2 h of electrolysis, indicating that applied potentials dramatically influence the H_2O_2 production. The H_2O_2 electrogeneration increases weakly with pH decrease due to the enhanced parasite reaction at anode in acidic solution. In the concentration range studied, the supporting electrolyte does not affect the net generation of H_2O_2 . Two-hour aeration with compressed air is required for the saturation of the solution in order to promote the H_2O_2 production. The modified cathode has much better performances on the degradation of Belgard EV 2030 than pristine under optimization parameters, indicating the positive effect of gold modification onto the electro-Fenton process.

References

- [1] E. Brillas, I. Sirés, M.A. Oturan, Electro-Fenton process and related electrochemical technologies based on Fenton's reaction chemistry, *Chem. Rev.* 109 (2009) 6570–6631.
- [2] N. Borràs, R. Oliver, C. Arias, E. Brillas, Degradation of atrazine by electrochemical advanced oxidation processes using a boron doped diamond anode, *J. Phys. Chem. A* 114 (2010) 6613–6621.
- [3] A. Dirany, I. Sirés, N. Oturan, M.A. Oturan, Electrochemical abatement of the antibiotic sulfamethoxazole from water, *Chemosphere* 81 (2010) 594–602.
- [4] C. Walling, A. Goosen, Mechanism of the ferric ion catalyzed decomposition of hydrogen peroxide. Effect of organic substrates, *J. Am. Chem. Soc.* 95 (1973) 2987–2991.
- [5] C. Walling, Fenton's reagent revisited, *Acc. Chem. Res.* 8 (1975) 125–131.
- [6] T. Rigg, W. Taylor, J. Weiss, The rate constant of the reaction between hydrogen peroxide and ferrous ions, *J. Chem. Phys.* 22 (1954) 575–577.
- [7] D.I. Metelista, Mechanism of the hydroxylation of aromatic compounds, *Russ. Chem. Rev.* 40 (1971) 563–580.
- [8] Y. Sun, J.J. Pignatello, Photochemical reactions involved in the total mineralization of 2,4-D by $\text{Fe}^{3+}/\text{H}_2\text{O}_2/\text{UV}$, *Environ. Sci. Technol.* 27 (1993) 304–310.
- [9] G.B. Buxton, C.L. Greenstock, W.P. Helman, A.B. Ross, Critical review of rate constants for reaction of hydrated electrons, hydrogen atoms and hydroxyl radicals ($\text{OH}^\bullet/\text{O}^{\bullet-}$) in aqueous solution, *J. Phys. Chem.* 17 (1988) 513–886.
- [10] S.S. Chou, Y.H. Huang, S.N. Lee, G.H. Huang, C.P. Huang, Treatment of high strength hexamine-containing wastewater by electro-Fenton method, *Water Res.* 33 (1999) 751–759.
- [11] E. Guinea, J.A. Garrido, R.M. Rodriguez, P.L. Cabot, C. Arias, F. Centellas, E. Brillas, Degradation of the fluoroquinolone enrofloxacin by electrochemical advanced oxidation processes based on hydrogen peroxide electrogeneration, *Electrochim. Acta* 55 (2010) 2101–2115.

- [12] E. Isarain-Chávez, J.A. Garrido, R.M. Rodriguez, F. Centellas, C. Arias, P.L. Cabot, E. Brillas, Mineralization of metoprolol by electro-Fenton and photo-electro-Fenton processes, *J. Phys Chem. A* 115 (2011) 1234–1242.
- [13] J.M. Peralta Hernández, Y. Meas-Vong, F.J. Rodríguez, T.W. Chapman, M.I. Maldonado, L.A. Godínez, In situ electrochemical and photo-electrochemical generation of the Fenton reagent: A potentially important new water treatment technology, *Water Res.* 40 (2006) 1754–1762.
- [14] K. Juttner, U. Galla, H. Schmieder, Electrochemical approaches to environmental problems in the process industry, *Electrochim. Acta* 45 (2000) 2575–2594.
- [15] C. Flox, P.L. Cabot, F. Centellas, J.A. Garrido, R.M. Rodriguez, C. Arias, E. Brillas, Solar photoelectro-Fenton degradation of Cresols using a flow reactor with a boron-doped diamond anode, *Appl. Catal., B* 75 (2007) 17–28.
- [16] E. Guivarch, N. Oturan, M.A. Oturan, Removal of organophosphorus pesticides from water by electro-generated Fenton's reagent, *Environ. Chem. Lett.* 1 (2003) 165–168.
- [17] M. Zhou, Q. Yu, L. Lei, The preparation and characterization of a graphite-PTFE cathode system for the decolorization of C.I. Acid Red 2, *Dyes Pigm.* 77 (2008) 129–136.
- [18] P. Drogui, S. Elmaleh, M. Rumeau, C. Bernard, A. Rambaud, Hydrogen peroxide production by water electrolysis: application to disinfection, *J. Appl. Electrochem.* 31 (2001) 877–882.
- [19] G. Zhang, F. Yang, L. Liu, Comparative study of $\text{Fe}^{2+}/\text{H}_2\text{O}_2$ and $\text{Fe}^{3+}/\text{H}_2\text{O}_2$ electro-oxidation systems in the degradation of amaranth using anthraquinone/polypyrrole composite film modified graphite cathode, *J. Electroanal. Chem.* 632 (2009) 154–161.
- [20] M.M. Ghoneim, H.S. El-Desoky, N.M. Zidan, Electro-Fenton oxidation of sunset yellow FCF azo-dye in aqueous solutions, *Desalination* 274 (2011) 22–30.
- [21] M. Panizza, G. Cerisola, Removal of organic pollutants from industrial wastewater by electrogenerated Fenton's reagent, *Water Res.* 35 (2001) 3987–3992.
- [22] E. Fokedey, A.V. Lierde, Coupling of anodic and cathodic reactions for phenol electro-oxidation using three-dimensional electrodes, *Water Res.* 36 (2002) 4169–4175.
- [23] M. Pimentel, N. Oturan, M. Dezotti, M.A. Oturan, Phenol degradation by advanced electrochemical oxidation process electro-Fenton using a carbon felt cathode, *Appl. Catal., B* 83 (2008) 140–149.
- [24] H. Wang, J.L. Wang, Electrochemical degradation of 4-chlorophenol using a novel Pd/C gas-diffusion electrode, *Appl. Catal., B* 77 (2007) 58–65.
- [25] H. Wang, J.L. Wang, Electrochemical degradation of 2,4-dichlorophenol on a palladium modified gas-diffusion electrode, *Electrochim. Acta* 53 (2008) 6402–6409.
- [26] W.B. Lu, C.X. Wang, Q.Y. Lv, X.H. Zhou, Electrocatalytic reduction of dioxygen on the surface of glassy carbon electrodes modified with dicobalt diporphyrin complexes, *J. Electroanal. Chem.* 558 (2003) 59–63.
- [27] J.C. Forti, R.S. Rocha, M.R.V. Lanza, R. Bertazzoli, Electrochemical synthesis of hydrogen peroxide on oxygen-fed graphite/PTFE electrodes modified by 2-ethylanthraquinone, *J. Electroanal. Chem.* 601 (2007) 63–67.
- [28] M.S. El-Deab, T. Okajima, T. Ohsaka, Electrochemical Reduction of oxygen on gold Nanoparticle Electrodeposited Glassy Carbon Electrodes, *J. Electrochem. Soc.* 150 (2003) A851–A857.
- [29] N. Al-Mutairi, F. Abdul Aleem, M.I. Al-Ahmad, Effect of antiscalants for inhibition of calcium sulfate deposition in thermal desalination systems, *Desalin. Water Treat.* 10 (2009) 39–46.
- [30] M.O. Finot, G.D. Braybook, M.T. McDermott, Characterization of electrochemically deposited gold nanocrystals on glassy carbon electrodes, *J. Electroanal. Chem.* 466 (1999) 234–241.
- [31] H. Martin, P. Carro, C. Hernandez, S. Ganzales, G. Andreasen, R.C. Salvaressa, A.J. Arvia, The influence of adsorbates on the growth mode of gold islands electrodeposited on the basal plane of graphite, *Langmuir* 16 (2000) 2915–2923.
- [32] G. Gunawardena, G. Hills, I. Montenegro, B. Scharifker, Electrochemical nucleation: Part I, *J. Electroanal. Chem. Interfacial Electrochem.* 138 (1982) 225–239.
- [33] G. Gunawardena, G. Hills, I. Montenegro, Electrochemical nucleation: Part II. The electrodeposition of silver on vitreous carbon, *J. Electroanal. Chem. Interfacial Electrochem.* 138 (1982) 241–254.
- [34] S.B. Brummer, A.C. Makrides, Surface oxidation of gold electrodes, *J. Electrochem. Soc.* 111 (1964) 1122.
- [35] Z. Qiang, J.H. Chang, Electrochemical generation of hydrogen peroxide from dissolved oxygen in acidic solutions, *Water Res.* 36 (2002) 85–94.
- [36] C.H. Chu, The electrochemical oxidation of recalcitrant organic compounds, PhD dissertation, University of Delaware, Newark, DE, 1995.
- [37] Y.H. Hsiao, K. Nobe, Hydroxylation of chlorobenzene and phenol in a packed bed flow reactor with electro-generated Fenton's reagent, *J. Appl. Electrochem.* 23 (1993) 943–946.
- [38] M.A. Oturan, J. Pinson, Hydroxylation by electrochemically generated OH radicals. Mono- and polyhydroxylation of benzoic acid: products and isomer distribution New, *J. Chem.* 16 (1992) 705–710.
- [39] T. Tzedakis, A. Savall, M.J. Clifton, The electrochemical regeneration of Fenton's reagent in the hydroxylation of aromatic substrates: batch and continuous processes, *J. Appl. Electrochem.* 19 (1989) 911–921.
- [40] Y. Sun, J.J. Pignatello, Photochemical reactions involved in the total mineralization of 2,4-D by iron (3+)/hydrogen peroxide/UV, *Environ. Sci. Technol.* 27 (1993) 304–310.
- [41] M.C. Edelhi, Contribution à l'étude de dégradation *in situ* des pesticides par procédés d'oxydation avancés faisant intervenir le fer, Application aux herbicides phénylurées. Doctorat de l'université de Marne-La-Vallée, Université de Marne-La-Vallée, 2004.